Monthly Notices
of the
ROYAL ASTRONOMICAL SOCIETY

MNRAS **468,** 1117–1122 (2017)
Advance Access publication 2017 March 1

doi:10.1093/mnras/stx525

An assessment of Fe XX–Fe XXII emission lines in SDO/EVE data as diagnostics for high-density solar flare plasmas using *EUVE* stellar observations

F. P. Keenan,[1⋆] R. O. Milligan,[1,2,3] M. Mathioudakis[1] and D. J. Christian[4]

[1]*Astrophysics Research Centre, School of Mathematics and Physics, Queen's University Belfast, BT7 1NN, UK*
[2]*Department of Physics, Catholic University of America, 620 Michigan Ave. NE, Washington DC 20064, USA*
[3]*Solar Physics Laboratory (Code 671), Heliophysics Science Division, NASA Goddard Space Flight Center, Greenbelt, MD 20771, USA*
[4]*Department of Physics and Astronomy, California State University, Northridge, CA 91330, USA*

Accepted 2017 February 27. Received 2017 February 7; in original form 2016 December 22

ABSTRACT

The Extreme Ultraviolet Variability Experiment (EVE) on the Solar Dynamics Observatory obtains extreme-ultraviolet (EUV) spectra of the full-disc Sun at a spectral resolution of ∼1 Å and cadence of 10 s. Such a spectral resolution would normally be considered to be too low for the reliable determination of electron density (N_e) sensitive emission line intensity ratios, due to blending. However, previous work has shown that a limited number of Fe XXI features in the 90–160 Å wavelength region of EVE do provide useful N_e-diagnostics at relatively low flare densities ($N_e \simeq 10^{11}$–10^{12} cm^{-3}). Here, we investigate if additional highly ionized Fe line ratios in the EVE 90–160 Å range may be reliably employed as N_e-diagnostics. In particular, the potential for such diagnostics to provide density estimates for high N_e ($\sim 10^{13}$ cm^{-3}) flare plasmas is assessed. Our study employs EVE spectra for X-class flares, combined with observations of highly active late-type stars from the *EUVE* satellite plus experimental data for well-diagnosed tokamak plasmas, both of which are similar in wavelength coverage and spectral resolution to those from EVE. Several ratios are identified in EVE data, which yield consistent values of electron density, including Fe XX 113.35/121.85 and Fe XXII 114.41/135.79, with confidence in their reliability as N_e-diagnostics provided by the *EUVE* and tokamak results. These ratios also allow the determination of density in solar flare plasmas up to values of $\sim 10^{13}$ cm^{-3}.

Key words: sun: corona – sun: flares – stars: coronae – stars: flare.

1 INTRODUCTION

Electron density (N_e) is a fundamental physical parameter of a plasma, and one of the main ways for determining this quantity in remote astrophysical sources is through emission-line intensity ratios, which are sensitive to variations in N_e. In the case of the high temperature solar transition region and corona, many of the emission lines lie at extreme-ultraviolet (EUV) wavelengths (∼100–1200 Å), and for more than half a century numerous researchers have worked on the calculation of theoretical line ratio N_e-diagnostics involving EUV transitions (see for example, Jordan 1966; Keenan 1996; Del Zanna & Badnell 2016). Such diagnostics have generally been used in conjunction with medium-to-high spectral resolution solar observations obtained with rocket-borne or satellite-based instrumentation, required to adequately resolve and hence reliably measure the relevant emission lines. Examples include the S082A instrument on board the Skylab space station, which had a resolution of ∼0.1 Å (Dere 1978), the Solar EUV Rocket Telescope and Spectrograph at 0.05–0.08 Å resolution (Thomas & Neupert 1994), the Coronal Diagnostic Spectrometer on the Solar and Heliospheric Observatory satellite at ∼0.4 Å resolution (Harrison et al. 1997) and the EUV Imaging Spectrometer on the Hinode satellite at ∼0.07 Å resolution (Young et al. 2007).

The Solar Dynamics Observatory (SDO), launched on 2010 February 11, contains a number of instruments including the Extreme Ultraviolet Variability Experiment (EVE), which obtains a full-disc EUV spectrum every 10 s using its MEGS-A component, albeit at a relatively low resolution of ∼1 Å (Woods et al. 2011). Although the EVE temporal resolution is unprecedented for an EUV spectrometer, allowing detailed studies of time-dependent phenomena such as flares, one would expect the spectral resolution to be too low to provide reliable electron density diagnostics. However, Milligan et al. (2012) found that a few Fe XXI emission-line ratios

⋆ E-mail: F.Keenan@qub.ac.uk

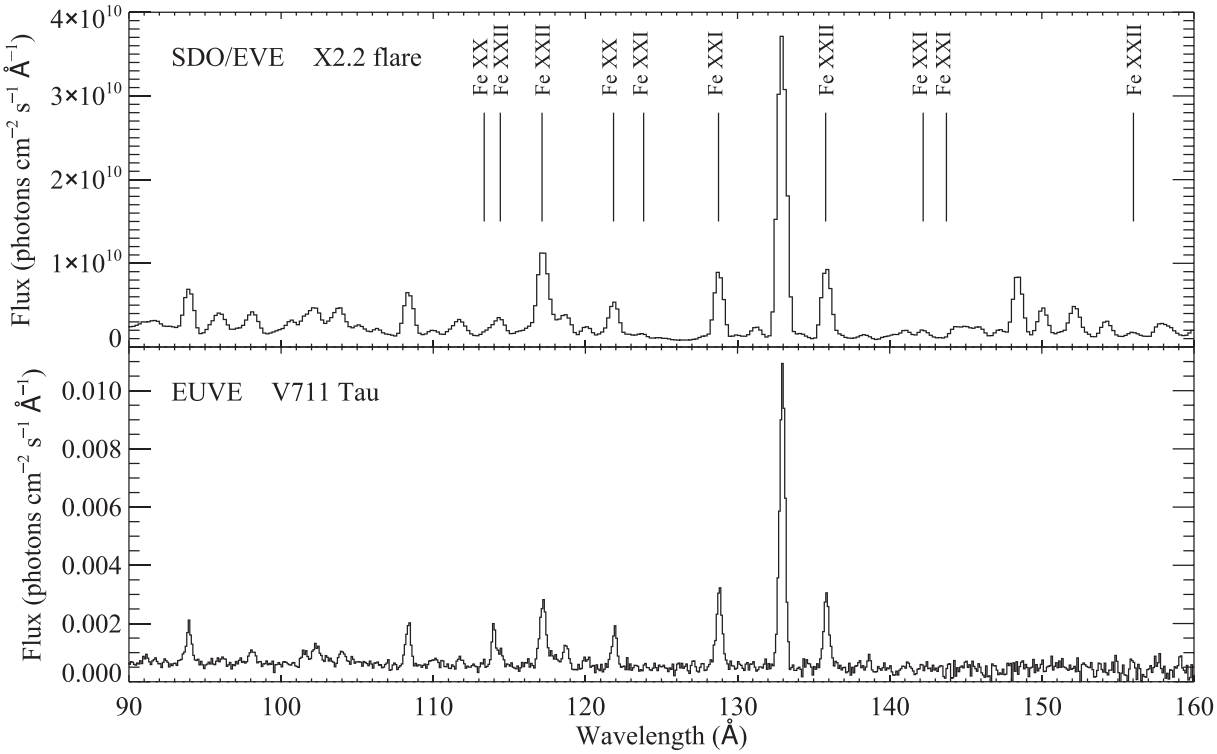

Figure 1. Comparison of the SDO/EVE spectrum of the solar flare of 2011 February 15 at 01:55:32 UT in the 90–160 Å wavelength range with that of the RS CVn star V711 Tau, obtained with the *EUVE* satellite. Several of the stronger, highly ionized Fe lines present in these spectra are marked.

in the 90–160 Å portion of the MEGS-A flare spectra provide useful electron density diagnostics for values of N_e in the range of $\sim 10^{11}$–10^{12} cm^{-3}; hence, allowing the study of the temporal evolution of relatively low flare density.

The short-wavelength (SW) spectrometer on the *Extreme Ultraviolet Explorer (EUVE)* satellite obtained spectra of astrophysical sources in the 70–190 Å region at a resolution of ∼0.5 Å (Abbott et al. 1996). It observed many highly-active late-type stars (see for example, Craig et al. 1997), and due to the comparable spectral coverage and resolution with EVE flare data, the *EUVE* and EVE observations can appear remarkably similar in terms of the presence of highly ionized Fe lines, as illustrated in Fig. 1. Hence, the *EUVE* spectra may be employed as a 'testbed' for Fe ion line ratio diagnostics in EVE observations, and, in particular, allow us to assess the potential usefulness of such diagnostics for high N_e flare plasmas, as active late-type stars can contain high-density (up to $\sim 10^{13}$ cm^{-3} or greater) coronal material.

In this paper, we significantly expand upon the work of Milligan et al. (2012) to establish if other high temperature (>10 MK) Fe lines apart from those of Fe XXI can be used to derived plasma densities under flare conditions. Specifically, we undertake a comparison of EVE and *EUVE* observations, plus published results for well-diagnosed high-density tokamak plasmas, to test the validity of additional highly ionized Fe line ratios present in EVE spectra between 90–160 Å as reasonable density diagnostics for flaring plasmas. More importantly, we also assess if they can be employed to derive densities in the high N_e ($\simeq 10^{12}$–10^{13} cm^{-3}) regime.

2 OBSERVATIONAL DATA

The solar observations considered in this paper consist of EVE spectra for two X-class solar flares obtained at event peak, namely that of 2011 February 15 at 01:55:32 UT (X2.2 class) and 2011 August 9 at 08:05:07 UT (X6.9 class). These flares were selected to maximize both the intensities of the highly ionized Fe lines of interest (and hence minimize the effect of blending from low temperature transitions), and the electron density of the emitting plasma (ideally reaching densities close to 10^{13} cm^{-3}). Details of the EVE instrument and data reduction procedures may be found in Woods et al. (2012) and Milligan et al. (2012). Briefly, the Multiple EUV Grating Spectrograph (MEGS)-A of EVE obtains full-disc spectra of the Sun in the 65–370 Å wavelength range, at a resolution of ∼1.0 Å, every 10 s. We have employed the most recent release of the EVE data (Level 2, Version 5), based on new rocket calibration flights, which improves the accuracy in the irradiance values presented in earlier releases (Milligan et al. 2012).

Our paper is focused on the ∼90–160 Å region of MEGS-A, which contained numerous emission lines arising from transitions in Fe XVIII–Fe XXIII. Del Zanna & Woods (2013) have previously undertaken an analysis of Fe XVIII–Fe XXIV features in EVE spectra, to investigate which of these may be relatively free of blending in solar flares and hence have the potential to be employed as diagnostics. However, these authors did not consider electron density diagnostics in detail, in particular the consistency of densities derived from different line ratios. Furthermore, they focused on plasmas with N_e in the range of $\sim 10^{11}$–10^{12} cm^{-3}, where many of the Fe line diagnostics are not particularly useful. For example, the Fe XXI (142.14 + 142.28)/128.75 ratio recommended by Milligan et al. (2012) only varies by ∼35 per cent between 10^{11} and 10^{12} cm^{-3}. The Fe XXI 145.73/128.75 ratio recommended by both Milligan et al. (2012) and Del Zanna & Woods varies by a much greater amount over this density interval (a factor of 4.8), but with the problem that the 145.73 Å line is very weak at such values of N_e, being predicted to be typically only

Table 1. Highly ionized Fe lines considered in the present analysis.

Species	Transition	Wavelength (Å)
Fe XX	$2s^2 2p^3\ ^2D_{5/2}–2s2p^4\ ^2D_{5/2}$	113.35
Fe XX	$2s^2 2p^3\ ^4S_{3/2}–2s2p^4\ ^4P_{3/2}$	121.85
Fe XXI	$2s^2 2p^2\ ^3P_2–2s2p^3\ ^3P_1$	123.83
Fe XXI	$2s^2 2p^2\ ^3P_0–2s2p^3\ ^3D_1$	128.75
Fe XXI	$2s^2 2p^2\ ^3P_1–2s2p^3\ ^3D_{1,2}$	142.14 + 142.28
Fe XXI	$2s^2 2p^2\ ^3P_2–2s2p^3\ ^3D_3$	145.73
Fe XXII	$2s^2 2p\ ^2P_{3/2}–2s2p^2\ ^2P_{3/2}$	114.41
Fe XXII	$2s^2 2p\ ^2P_{1/2}–2s2p^2\ ^2P_{1/2}$	117.15
Fe XXII	$2s^2 2p\ ^2P_{1/2}–2s2p^2\ ^2D_{3/2}$	135.79
Fe XXII	$2s^2 2p\ ^2P_{3/2}–2s2p^2\ ^2D_{5/2}$	156.02

5 per cent of the intensity of 128.75 Å. By contrast, our work is primarily concerned with the identification and assessment of diagnostics for much higher density flare plasmas, ideally up to $N_e \simeq 10^{13}$ cm^{-3} or even greater.

In Table 1, we summarize the lines judged by Del Zanna & Woods (2013) to be blend free and which may provide electron density sensitive intensity ratios. However, in addition, we include the Fe XXI 123.83 and Fe XXII 156.02 Å transitions. The former was not considered by Del Zanna & Woods, while in the case of Fe XXII 156.02 Å these authors noted that the line appeared to be blended as it implied a very high value of electron density. To investigate the potential blending of these features, we have calculated synthetic spectra with the latest version (8.0.1) of the CHIANTI collisional-radiative modelling packages, appropriate for plasmas with densities up to $\sim 10^{15}$ cm^{-3} (Dere et al. 1997; Del Zanna et al. 2015). Spectra have been generated for electron densities in the range of 10^{11}–10^{13} cm^{-3}, and for the standard CHIANTI flare differential emission measure (DEM) distribution. Although each solar flare will have its own characteristics (including DEM), we note that the highly ionized Fe lines are formed over a narrow range of temperatures of maximum fractional abundance, log T_{max} = 7.0–7.1 (Bryans, Landi & Savin 2009). The DEMs of different flares do not vary significantly over this temperature interval, as shown by, for example, fig. 5 of Kennedy et al. (2013). Our CHIANTI synthetic spectra indicate that blending species (primarily Cr XVII 122.97, Mn XXI 124.08 and Cr XX 156.02 Å) should make at most ∼25 per cent contributions to the total measured line fluxes of both the Fe XXI 123.83 and Fe XXII 156.02 Å lines.

For late-type stellar observations, we have employed spectra from the *EUVE* satellite mission, which operated from 1992 June 7 to 2001 January 31. A full description of the *EUVE* spectrometers may be found in Abbott et al. (1996) and references therein. Briefly, *EUVE* observed sources over the 70–760 Å wavelength range using three slitless, imaging spectrometers, with that of relevance to the present paper being the SW instrument which covered 70–190 Å at a resolution of ∼0.5 Å. An atlas of the spectra for 95 stellar sources from the *EUVE* Public Archive was published in Craig et al. (1997), which also contains details of the data reduction procedures. We have selected a sample of late-type stars for our study which are extremely active and hence show strong emission from highly ionized Fe lines, as well as large electron density estimates ($N_e > 10^{12}$ cm^{-3}) for the emitting coronal plasma. Data for these objects were obtained from the Mikulski Archive for Space Telescopes (MAST). The archival spectra were processed with *EUVE* IRAF software version 1.9 with reference data EGODATA 1.17, and analysed using IRAF and custom IDL routines. To improve the signal-to-noise ratio of the *EUVE* data, we created new summed data sets using all available SW observations in MAST for UX Ari (4 spectra), V711 Tau (7) and AD Leo (9), while for 44i Boo and AU Mic we analysed existing co-added data. The total exposure times of the summed *EUVE* spectra are listed in Table 2. Detailed information on each star and the relevant *EUVE* spectral data sets may be found in the following references: Brickhouse & Dupree (1998) for 44i Boo, Monsignori Fossi et al. (1996) for AU Mic, Sanz-Forcada, Brickhouse & Dupree (2002) for UX Ari and V711 Tau and Sanz-Forcada & Micela (2002) for AD Leo.

The final sets of EUV spectra considered here are from the Frascati Tokamak Upgrade (FTU) and Princeton Large Torus (PLT) tokamaks, obtained by Fournier et al. (2001) and Stratton, Moos & Finkenthal (1984), Stratton et al. (1985), respectively. All three data sets have a spectral resolution of ∼0.7 Å, similar to those of the EVE and *EUVE* observations. The tokamak spectra will not show the same level of blending as the astrophysical data, due to the latter sampling a larger number of elements. However, they should still provide a useful comparison with the solar/stellar observations, as most of the significant emission lines in the EUV region of interest arise from other high-ionization Fe transitions. This is shown by, for example, a comparison of the Fe spectrum of the FTU tokamak between 85 and 140 Å in fig. 2 of Fournier et al. (2001) with the EVE and *EUVE* data in Fig. 1, which appear very similar. Hence, the tokamak spectra should allow the reliability and consistency of highly ionized Fe line diagnostics to be assessed. Tokamaks are also particularly useful to this study, as their plasmas have very large values of N_e, similar to or greater than those of high-electron density flares.

3 RESULTS AND DISCUSSION

Line fluxes for the Fe ion lines in both the EVE and *EUVE* spectra were determined by fitting multiple Gaussian profiles to the observations, with some example fits shown in Figs 2 and 3. The resultant line intensity ratios (in photon units), along with the $\pm 1\sigma$ errors, are listed in Table 2. Also included in the table are the observed line ratios for the FTU and PLT tokamak spectra, taken directly from Fournier et al. (2001) and Stratton et al. (1984, 1985).

We have derived values of electron density from the observed EVE, *EUVE* and tokamak line ratios using theoretical results from the latest version (8.0.1) of CHIANTI (Dere et al. 1997; Del Zanna et al. 2015). All of the line ratio calculations were performed at the value of T_{max} of the relevant Fe ion (Bryans et al. 2009), although we note that the results are not sensitive to the adopted temperature. For example, changing the electron temperature for the Fe XXI (142.14 + 142.28)/128.75 line ratio calculations from $T_{max} = 1.1 \times 10^7$ K to 2×10^7 K leads to a <0.1 dex variation in the derived value of N_e. Similarly, for Fe XXII 114.41/135.79, adopting $T_e = 2.5 \times 10^7$ K rather than $T_{max} = 1.3 \times 10^7$ K also results in a < 0.1 dex change in the density estimate. Hence, even if the plasma is not in ionization equilibrium and the temperature is significantly different from T_{max}, as may be the case during a flare (see for example, Kawate, Keenan & Jess 2016), this should not affect the derived values of N_e. Furthermore, the time-scale to achieve ionization equilibrium scales with electron density, and for the high N_e events considered here the ionization state of Fe should be close to equilibrium (Bradshaw 2009).

Also listed in Table 2 are the electron densities, denoted N_e (other), determined from a range of high-temperature ions in the *EUVE* spectra, in particular, those with lines known to be blended in the EVE spectra (Del Zanna & Woods 2013) but which should be relatively unblended in the (somewhat) greater resolution *EUVE* observations. These include density diagnostics such as Fe XX

Table 2. Fe ion line intensity ratios[a] and derived logarithmic electron densities.

Line ratio	2011 February 15 flare 01:55:32 UT	2011 August 9 flare 08:05:07 UT	44i Boo 141 ks[b]	AU Mic 69.6 ks[b]	UX Ari 450 ks[b]	V711 Tau 790 ks[b]	AD Leo 1100 ks[b]	FTU tokamak[c]	PLT tokamak[d]	PLT tokamak[d]	PLT tokamak[e]
Fe XX 113.35/121.85	...	0.20 ± 0.02	0.21 ± 0.12	0.23 ± 0.14	0.16 ± 0.10	0.18 ± 0.12	0.25 ± 0.17	...	...	...	...
	...	12.6 ± 0.1	$12.7^{+0.5}_{-0.9}$	$12.8^{+0.5}_{-1.0}$	$12.4^{+0.5}_{-1.2}$	$12.5^{+0.6}_{-1.3}$	$12.9^{+0.6}_{-1.2}$	...	...	...	...
Fe XXI (142.14 + 142.28)/128.75	0.13 ± 0.02	0.16 ± 0.02	0.51 ± 0.24	0.21 ± 0.11	0.29 ± 0.15	0.17 ± 0.07	0.38 ± 0.17	1.3 ± 0.2	...	...	0.91
	$11.7^{+0.2}_{-0.6}$	$12.0^{+0.1}_{-0.2}$	$12.9^{+0.3}_{-0.4}$	$12.3^{+0.3}_{-1.7}$	$12.5^{+0.3}_{-0.7}$	$12.0^{+0.4}_{-1.4}$	$12.7^{+0.3}_{-0.4}$	$13.8^{+0.3}_{-0.2}$	...	...	13.4
Fe XXI 145.73/128.75	0.21 ± 0.04	0.17 ± 0.03	0.34 ± 0.19	0.22 ± 0.06	0.11 ± 0.09	0.05 ± 0.02	0.06 ± 0.03	1.0 ± 0.2	...	...	0.61
	$12.4^{+0.1}_{-0.2}$	12.2 ± 0.1	$12.7^{+0.4}_{-0.6}$	$12.4^{+0.2}_{-0.2}$	$12.0^{+0.3}_{-1.2}$	$11.5^{+0.2}_{-0.4}$	$11.6^{+0.2}_{-0.5}$	$13.7^{+0.3}_{-0.3}$	...	...	13.2
Fe XXI 123.83/(142.14 + 142.28)	0.91 ± 0.17	0.49 ± 0.06	0.37 ± 0.08	0.64 ± 0.41	0.50 ± 0.37	0.20 ± 0.11	0.28 ± 0.19	...	...	...	...
	L[f]	L[f]	<10.0	<11.8	<12.7	$12.1^{-\infty}_{+1.6}$	$10.9^{-\infty}_{+2.8}$	...	...	...	...
Fe XXII 114.41/135.79	0.25 ± 0.03	0.25 ± 0.02	0.41 ± 0.23	0.26 ± 0.09	0.29 ± 0.11	0.21 ± 0.04	0.30 ± 0.08	...	0.79	0.60	0.82
	$12.5^{+0.2}_{-0.3}$	$12.5^{+0.2}_{-0.1}$	$13.1^{+0.4}_{-\infty}$	$12.6^{+0.4}_{-\infty}$	$12.8^{+0.3}_{-\infty}$	$12.1^{+0.4}_{-\infty}$	$12.8^{+0.3}_{-0.6}$	...	13.7	13.5	13.8
Fe XXII 114.41/117.15	0.17 ± 0.02	0.25 ± 0.02	0.54 ± 0.30	0.22 ± 0.08	0.23 ± 0.07	0.23 ± 0.07	0.24 ± 0.04	1.1 ± 0.3	0.67	0.33	0.40
	<11.4	$12.6^{+0.1}_{-0.2}$	$13.4^{+0.4}_{-0.9}$	$12.3^{+0.5}_{-\infty}$	$12.4^{+0.4}_{-\infty}$	$12.4^{+0.4}_{-\infty}$	$12.5^{+0.2}_{-0.6}$	$14.1^{+0.5}_{-0.3}$	13.6	12.9	13.1
Fe XXII 156.02/135.79	0.14 ± 0.04	0.076 ± 0.013	0.18 ± 0.14	0.29 ± 0.07	0.19 ± 0.12	0.19 ± 0.16	0.21 ± 0.10	0.55 ± 0.06	...	...	0.59
	$12.9^{+0.1}_{-0.3}$	$12.4^{+0.1}_{-0.2}$	$13.0^{+0.4}_{-\infty}$	$13.4^{+0.1}_{-0.2}$	$13.1^{+0.3}_{-0.8}$	$13.1^{+0.2}_{-0.3}$	$13.1^{+0.3}_{-0.4}$	$13.8^{+0.1}_{-0.1}$	...	...	13.9
Mean density	12.4 ± 0.5	12.4 ± 0.2	13.0 ± 0.3	12.6 ± 0.4	12.5 ± 0.4	12.3 ± 0.5	12.6 ± 0.5	13.9 ± 0.2	13.7 ± 0.1	13.2 ± 0.4	13.5 ± 0.4
Log N_e (other)[g]	...	...	13.2 ± 0.7	12.7 ± 0.5	12.5 ± 0.4	12.2 ± 0.1	12.9 ± 0.3	13.9	13.5	12.7	13.4

Notes. [a]Ratios are in photon units.
[b]Total exposure time of the summed *EUVE* short-wavelength spectrum.
[c]From Fournier et al. (2001).
[d]From Stratton et al. (1984).
[e]From Stratton et al. (1985).
[f]L indicates that the observed ratio is greater than the theoretical low-density limit.
[g]Stellar electron densities derived from a range of high-temperature ions in the *EUVE* spectra. The tokamak values are those measured by Fournier et al. (2001) or Stratton et al. (1984, 1985).

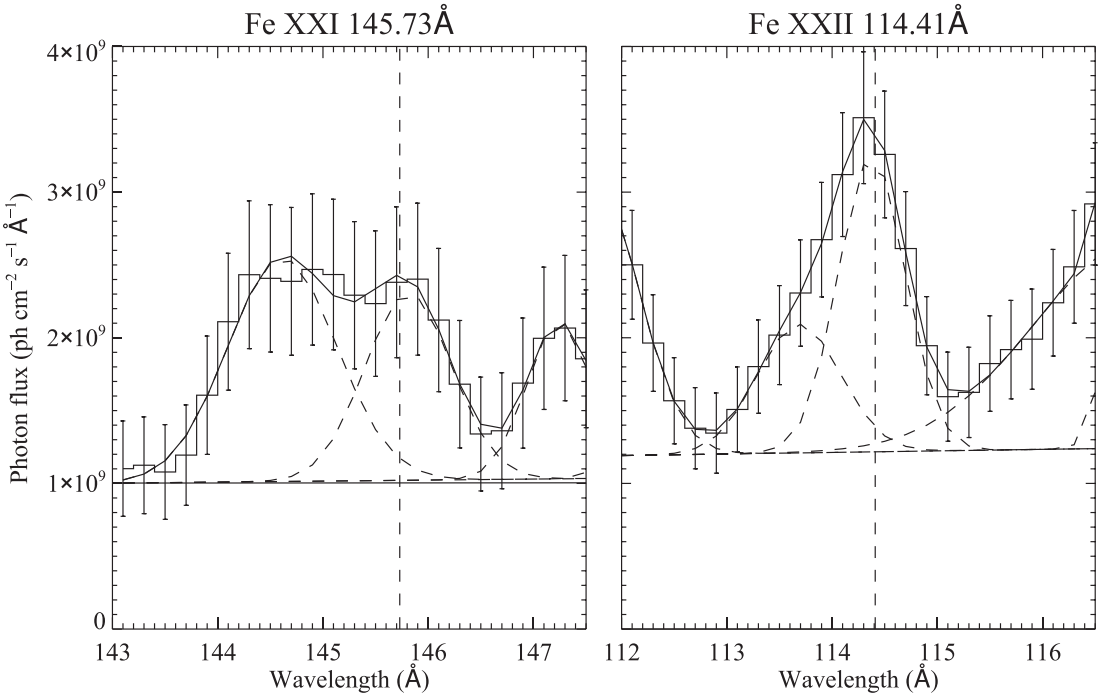

Figure 2. Portions of the EVE spectrum for the 2015 February 15 solar flare at 01:55:32 UT, showing the Fe XXI 145.73 and Fe XXII 114.41 Å emission features, both marked with vertical dashed lines. Also shown with dashed lines are the multiline fits to the profiles, which include emission features due to Ca XV 144.31 + Fe XXIII 144.39 Å, Fe XXIII 147.25 Å and Fe XXI 113.29 + Fe XX 113.35 Å, plus the wings of Fe XIX 111.70 + Ni XXIII 111.83 Åand Fe XXII 117.15 Å.

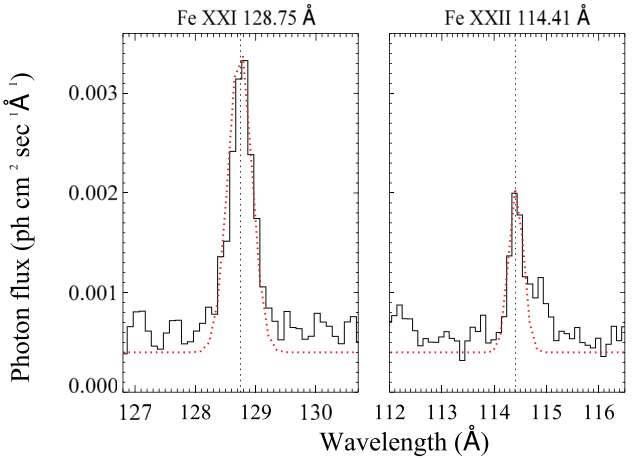

Figure 3. Portions of the *EUVE* Short Wavelength (SW) spectrometer observations for the RS CVn star V711 Tau, with a total exposure time of 790 ks, obtained during the period 1992 October 22 to 1999 September 13. Profile fits to the Fe XXI 128.75 Å and Fe XXII 114.41 Å emission features are shown as dashed lines.

121.85/110.63, Fe XXI 121.21/128.75 and Fe XXII 116.27/117.15. For the tokamak observations, N_e (other) is the experimental plasma density, determined from interferometry measurements to an accuracy of approximately ±15 per cent (Stratton et al. 1984, 1985; Fournier et al. 2001).

The first point to note from an inspection of Table 2 is that the Fe XXI 123.83 Å line is clearly blended to a very significant degree in the EVE observations, as the measured values of Fe XXI 123.83/(142.14 + 142.28) are both far greater (by factors of 1.7 and 3.1) than the theoretical low density limit of 0.29. As noted in Section 2, this line was not considered by Del Zanna & Woods (2013) in their assessment of EVE flare data, although it is not predicted to be severely blended. However, blending species must make a much larger contribution to the total intensity than evisaged, including perhaps unidentified transitions.

For the other Fe ion lines in the EVE spectra, the resultant intensity ratios imply electron densities that are reasonably consistent, with discrepancies that average only 0.3 dex from the mean value of log $N_e = 12.4$ for both flares. Similarly, for the *EUVE* data sets, the line ratios lead to electron density estimates for each star that are consistent within the errors, and indicate average densities which show no significant discrepancies with those derived from a wider range of high temperature N_e-diagnostic lines. Differences between the mean densities and the values of N_e (other) average only 0.1 dex, and do not exceed 0.3 dex. We note that as the *EUVE* spectra analysed here are the sum of several SW data sets, the derived densities will not represent specific flare values, but rather time-averaged estimates over the duration of the observations. However, this is not an issue as we are only concerned with the consistency of densities derived from different line ratios, and hence a comparison of time-averaged values is appropriate. In addition, it is worth pointing out that the ratio values for individual flares are actually very similar to those from the summed spectra. For example, for AU Mic the measured Fe XXII 114.41/135.79 and 114.41/117.15 ratios in Table 2 are 0.26 and 0.22, respectively, while those for a specific flare (interval b of Monsignori Fossi et al. 1996) are 0.30 and 0.23. The similar ratio values reflect the fact that the spectral emission is dominated, as might be expected, by high-density flaring plasma. However, we employ summed *EUVE* spectra in our work, as these provide better signal-to-noise ratio and hence more reliable detections, especially for weak features.

In the case of the tokamak spectra, the derived average values of N_e are consistent with the experimental data in three out of four instances, with discrepancies of less than 0.2 dex. The exception

is the PLT data of Stratton et al. (1984) at an experimental density of log N_e = 12.7, where the diagnostics indicate log N_e = 13.2 ± 0.4. This is due to the Fe XXII 114.41/135.79 ratio being much larger than expected; the measured value is 0.60, while for an experimental density of log N_e = 12.7 the theoretical ratio is only 0.28. Stratton et al. (1984) also noted this discrepancy, and it remains unexplained. However, the problem must lie with the 135.79 Å line measurement in the spectrum, as the Fe XXII 114.41/117.15 ratio shows no significant differences between theory (0.27 at log N_e = 12.7) and observation (0.33), and hence the 114.41 Å experimental intensity should be secure. We note that there is no issue with the 135.79 Å line in the FTU spectrum of Fournier et al. (2001), with good agreement between the density derived from Fe XXII 156.02/135.79 (log N_e = 13.8 ± 0.1) and the measured value (log N_e = 13.9). Furthermore, there is consistency between theory and observation for Fe XXII 114.41/135.79 in the PLT spectrum for the log N_e = 13.5 plasma, with the measured value indicating log N_e = 13.7, providing support for the reliability of the CHIANTI line ratio calculations.

4 CONCLUSIONS

The consistency of the electron densities determined from the EVE observations, combined with that also found from the *EUVE* and tokamak data of similar spectral resolution, indicates that the line ratios in Table 2 with the exception of Fe XXI 123.83/(142.14 + 142.28) should provide reasonable estimates of N_e for the high temperature (∼10 MK) plasma in solar flares. More importantly, the *EUVE* and tokamak results provide support for the line ratio diagnostics being reliable up to very high values of N_e ($\simeq 10^{13}$ cm^{-3}), and confirm the large densities derived for the solar events. Milligan et al. (2012) found that two of the Fe XXI ratios in Table 2 – 145.73/128.75 and (142.14 + 142.28)/128.75 – provided good estimates of density at $N_e \simeq 10^{12}$ cm^{-3}. (We note in passing that these authors also considered Fe XXI 121.21/128.75, which we exclude as Del Zanna & Woods (2013) point out that the 121.21 Å feature is very weak and in the wing of the strong Fe XX 121.84 Å line). However, this work significantly extends the Milligan et al. (2012) analysis to show that four additional ratios of Fe XX and Fe XXII may be confidently used as diagnostics, even at the low spectral resolution of EVE, and furthermore allow a high-electron density regime to be reliably investigated. As EVE obtains full-disc spectra at a very high cadence of 10 s (as opposed to its low spectral resolution), this, in turn, indicates that the observations may be employed for reliable temporally resolved studies of flare densities in the high N_e regime (∼10^{12}–10^{13} cm^{-3}), and, in particular, the investigation of the maximum density that can be achieved during flare peak. The EVE instrument has observed hundreds of flares during its 4 yr of operation, providing a very large data set for such studies. Measurement of as many as possible of the line ratios in Table 2 would be preferred, as the average densities are in better agreement with N_e (other) than the individual values, which show a large amount of scatter. However, the best diagnostics – based on their density sensitivity particularly at high N_e, and how well the derived densities agree with N_e (other) – are probably Fe XX 113.35/121.85, Fe XXI (142.14 + 142.28)/128.75 and Fe XXII 114.41/135.79.

Now that we have confirmed the usefulness of MEGS-A data for determining high flare densities, the next step is to extend our analyses to the MEGS-B spectral region (350–1050 Å), which samples lower temperature emission lines. The overall aim of this work will be to identify diagnostics which allow time profiles of flare densities simultaneously across a broad temperature range (∼0.1–10 MK).

ACKNOWLEDGEMENTS

FPK and MM are grateful to the Science and Technology Facilities Council for financial support. The research leading to these results has received funding from the European Community's Seventh Framework Programme (FP7/2007-2013) under grant agreement no. 606862 (F-CHROMA). We are also grateful to the Leverhulme Trust for financial support via grant F/00203/X. ROM acknowledges support from NASA LWS/SDO Data Analysis grant NNX14AE07G. CHIANTI is a collaborative project involving George Mason University, the University of Michigan (USA) and the University of Cambridge (UK). The *EUVE* data presented in this paper were obtained from the MAST. STScI is operated by the Association of Universities for Research in Astronomy, Inc., under NASA contract NAS5-26555. Support for MAST for non-HST data is provided by the NASA Office of Space Science via grant NNX09AF08G and by other grants and contracts.

REFERENCES

Abbott M. J., Boyd W. T., Jelinksy P., Christian C., Miller-Bagwell A., Lampton M., Malina R. F., Vallerga J. V., 1996, ApJS, 107, 451
Bradshaw S. J., 2009, A&A, 502, 409
Brickhouse N. S., Dupree A. K., 1998, ApJ, 502, 918
Bryans P., Landi E., Savin D. W., 2009, ApJ, 691, 1540
Craig N. et al., 1997, ApJS, 113, 131
Del Zanna G., Badnell N. R., 2016, A&A, 585, A118
Del Zanna G., Woods T. N., 2013, A&A, 555, A59
Del Zanna G., Dere K. P., Young P. R., Landi E., Mason H. E., 2015, A&A, 582, A56
Dere K. P., 1978, ApJ, 221, 1062
Dere K. P., Landi E., Mason H. E., Monsignori-Fossi B. C., Young P. R., 1997, A&AS, 125, 149
Fournier K. B., May M. J., Liedahl D. A., Pacella D., Finkenthal M., Leigheb M., Mattioli M., Goldstein W. H., 2001, ApJ, 561, 1144
Harrison R. A. et al., 1997, Sol. Phys., 170, 123
Jordan C., 1966, MNRAS, 132, 515
Kawate T., Keenan F. P., Jess D. B., 2016, ApJ, 826, 3
Keenan F. P., 1996, Space Sci. Rev., 75, 537
Kennedy M. B., Milligan R. O., Mathioudakis M., Keenan F. P., 2013, ApJ, 779, 84
Milligan R. O., Kennedy M. B., Mathioudakis M., Keenan F. P., 2012, ApJ, 755, L16
Monsignori Fossi B. C., Landini M., Del Zanna G., Bowyer S., 1996, ApJ, 466, 427
Sanz-Forcada J., Micela G., 2002, A&A, 394, 653
Sanz-Forcada J., Brickhouse N. S., Dupree A. K., 2002, ApJ, 570, 799
Stratton B. C., Moos H. W., Finkenthal M., 1984, ApJ, 279, L31
Stratton B. C., Moos H. W., Suckewer S., Feldman U., Seely J. F., Bhatia A. K., 1985, Phys. Rev. A, 31, 2534
Thomas R. J., Neupert W. M., 1994, ApJS, 91, 461
Woods T. N. et al., 2011, ApJ, 739, 59
Woods T. N. et al., 2012, Sol. Phys., 275, 115
Young P. R. et al., 2007, PASJ, 59, S857

This paper has been typeset from a TEX/LATEX file prepared by the author.